Chromatin decondensation and nuclear reorganization of the *HoxB* locus upon induction of transcription

Séverine Chambeyron and Wendy A. Bickmore[1]

MRC Human Genetics Unit, Edinburgh EH4 2XU, United Kingdom

The colinearity of genes in Hox clusters suggests a role for chromosome structure in gene regulation. We reveal programmed changes in chromatin structure and nuclear organization upon induction of *Hoxb* expression by retinoic acid. There is an early increase in the histone modifications that are marks of active chromatin at both the early expressed gene *Hoxb1*, and also at *Hoxb9* that is not expressed until much later. There is also a visible decondensation of the chromatin between *Hoxb1* and *Hoxb9* at this early stage. However, a further change in higher-order chromatin structure, looping out of genes from the chromosome territory, occurs in synchrony with the execution of the gene expression program. We suggest that higher-order chromatin structure regulates the expression of the *HoxB* cluster at several levels. Locus-wide changes in chromatin structure (histone modification and chromatin decondensation) may establish a transcriptionally poised state but are not sufficient for the temporal program of gene expression. The choreographed looping out of decondensed chromatin from chromosome territories may then allow for activation of high levels of transcription from the sequence of genes along the cluster.

[*Keywords*: Chromatin decondensation; chromosome territory; differentiation; gene expression; histone modification; nuclear structure]

Received November 18, 2003; revised version accepted April 2, 2004.

To understand how chromatin regulates gene expression it is necessary to analyze not only nucleosome structure and modifications but also higher-order chromatin condensation and nuclear organization. Many correlations between transcription and nucleosome modifications have been found. For example, active β-globin loci are enriched in hyperacetylated histones H3 and H4, and H3 dimethylated on lysine 4 (met_2H3-K4), whereas the silent domain flanking the chicken locus has hypoacetylated histones and H3 dimethylated on K9 (met_2H3-K9; Litt et al. 2001; Bulger et al. 2003; Kim and Dean 2003). How histone modifications influence transcription is still debated. They can act as binding sites for specific regulatory proteins (Fischle et al. 2003) and may directly affect higher-order chromatin structure and condensation (Tse et al. 1998; Wolffe and Hayes 1999; Carruthers and Hansen 2000; Wang et al. 2001).

Chromatin organization at and beyond the level of the 30-nm chromatin fiber is poorly understood. Cytologically, chromatin decondensation is seen at transcriptionally active regions in the polytene chromosomes of dipteran insects (Andersson et al. 1984) and when transcriptional regulators are artificially targeted to sites in the mammalian genome (Tumbar et al. 1999; Tsukamoto et al. 2000; Muller et al. 2001; Ye et al. 2001; Nye et al. 2002). It is not clear whether chromatin decondensation accompanies the induction of endogenous mammalian gene expression.

There is also a complex relationship between transcription and the position of genes within chromosome territories (CTs). Some studies show inactive genes located in the interior of CTs and active genes concentrated at the territory periphery (Kurz et al. 1996; Dietzel et al. 1999), but active genes can be transcribed from inside of CTs (Mahy et al. 2002b). Moreover, regions with a high density of coordinately expressed genes locate in loops that extend outside of CTs in expressing cells but not in nonexpressing cells (Volpi et al. 2000; Williams et al. 2002). Localization outside of CTs also occurs at genomic regions with a high-density of broadly expressed genes (Mahy et al. 2002a). Hence, it has been suggested that there is a correlation between high levels of transcriptional activity and localization outside of CTs (Mahy et al. 2002a).

It is not known whether chromatin decondensation and CT organization are just consequences of the changes in histone modifications accompanying gene activation, or whether they are independent levels of chromatin structure over and above the level of the nucleo-

[1]**Corresponding author.**
E-MAIL W.Bickmore@hgu.mrc.ac.uk; FAX 44-131-467-8456.
Article and publication are at http://www.genesdev.org/cgi/doi/10.1101/gad.292104.

some. At the mammalian β-globin locus, altered nuclear organization (movement away from heterochromatin) correlates with general histone acetylation and the LCR appears to be responsible for localizing the region outside of CTs prior to gene activation. These studies suggest that nuclear reorganization is upstream of histone modifications in a pathway to chromatin opening and that it is necessary to create a transcriptionally poised state that precedes gene expression (Schubeler et al. 2000; Ragoczy et al. 2003).

To understand the relationships between gene expression, nucleosome modification, chromatin decondensation, and nuclear organization, we have studied the developmentally regulated *Hoxb* gene cluster. Establishing correct spatial and temporal domains of *Hox* expression is important for anteroposterior (AP) patterning (Krumlauf 1994; Popperl et al. 1995; Studer et al. 1998). This is partly achieved through the colinearity of gene order along the chromosome, with the time and place of gene activation (Fig. 1A; for review, see Kmita and Duboule 2003). The mechanisms for vertebrate *Hox* gene regulation are largely unknown, but *cis*-acting regulatory elements (see Marshall et al. 1994; Popperl et al. 1995; Maconochie et al. 1997; Oosterveen et al. 2003), as well as higher-order silencing mechanisms (Kondo and Duboule 1999) are involved. A progressive transition from an inactive (closed) to an active (open) chromatin state, propagated through the cluster from 3′ to 5′, has been proposed (Van der Hoeven et al. 1996; Kondo and Duboule 1999; Roelen et al. 2002). These models are inferred from transgenic reporter approaches (see Marshall et al. 1994; Maconochie et al. 1997) and from rearrangements that reposition *Hox* genes within a cluster (Van der Hoeven et al. 1996; Kondo et al. 1998).

Given the interest in the control of *Hox* gene expression, it is surprising that little is known about their chromatin structure. By using retinoic acid (RA) to induce regulated expression of *Hoxb* genes in mouse embryonic stem (ES) cells, we have performed chromatin immunoprecipitation (ChIP) to track histone modifications, and fluorescence in situ hybridization (FISH) to analyze chromatin condensation and nuclear organization. Within 4 d of induction, there are increases in histone modifications associated with transcriptional activity (AcH3-K9 and met_2H3-K4) at both the early expressed *Hoxb1* and also at genes that will not be transcribed until later in the developmental program (*Hoxb9*). At this stage there is also a dramatic decondensation of the *HoxB* cluster, which is not a simple consequence of the increase in histone acetylation. There is then a choreographed extrusion of genes outside of CTs that is coincident with the temporal program of gene expression. We propose a two-step model for how chromatin structure regulates expression from *HoxB*. First a locus-wide change in chromatin structure (histone modification and chromatin decondensation) may create a transcriptionally poised

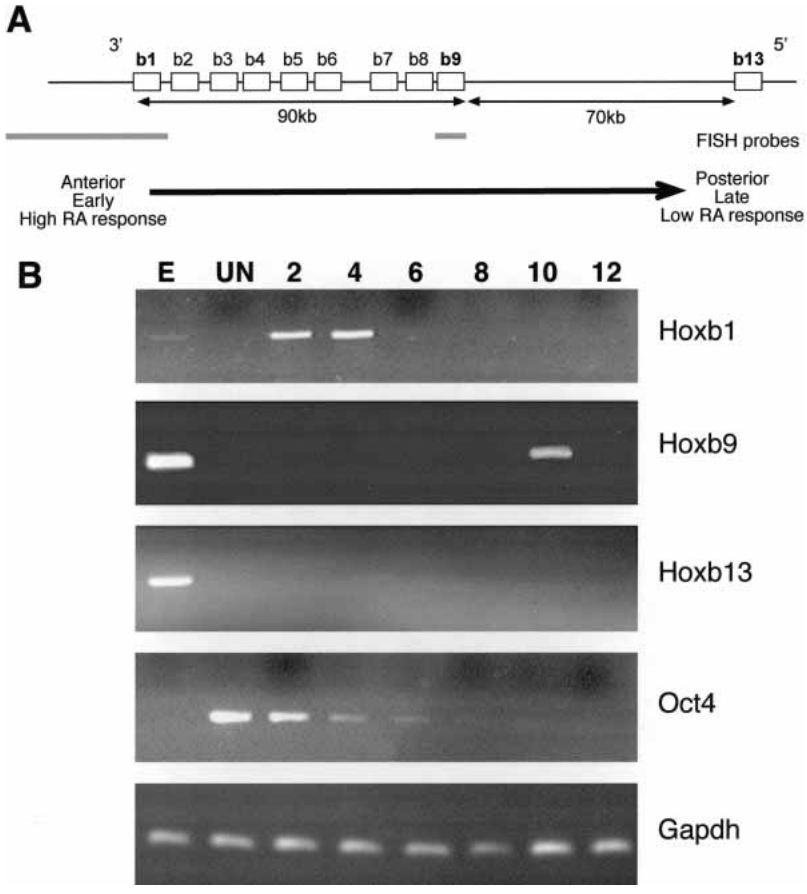

Figure 1. Organization and differential activation of the Hoxb locus in ES cells. (*A*) Chromosomal organization of genes (open boxes) in the murine *Hoxb* complex. 5′ and 3′ indicate the direction of the transcription. The distance between genes is indicated *below* the map, as is the position of FISH probes (gray bars) for *Hoxb1* and *Hoxb9*. The arrow indicates the colinear properties of the *Hoxb* cluster with respect to spatial expression (anterior to posterior), time of expression (early to late), and sensitivity to RA. Modified from Hunt and Krumlauf (1992). (*B*) Differential expression of *Hoxb* genes in OS25 ES cells. RT–PCR analysis of *Hoxb1*, *9*, and *13* in undifferentiated (UN) cells and in cells induced to differentiate with RA for 2 to 12 d. Differentiation was confirmed by the loss of *Oct4* expression. Total RNA from E11.5 embryo (E) and analysis of *Gapdh* were used as positive controls.

state. Then a progressive 3′ to 5′ change in higher-order chromatin structure, which is manifest as the movement outside of CTs, is necessary to allow for the programmed expression of genes along the cluster.

Results

RA induces a temporal program of Hoxb *gene expression in ES cells*

In vivo the activation of *Hox* gene expression by retinoids is mediated by *cis*-acting RA response elements (RAREs; for review, see Gavalas and Krumlauf 2000). *Hox* genes also show a colinear temporal response to RA ex vivo. In embryonal carcinoma cells, genes at the 3′ extremity of the clusters respond earlier, and at lower RA concentrations, than do more 5′ genes (Fig. 1A; Simeone et al. 1990, 1991; Papalopulu et al. 1991). RA also induces *Hox* expression in ES cells (Papalopulu et al. 1991). We induced expression of the *HoxB* cluster with RA in wild-type ES cells but obtained a nonhomogeneous response as revealed by the expression of SSEA-1 antigen in residual undifferentiated ES cells (Brown et al. 1993; data not shown). Because studies of nuclear organization rely on analysis at the single cell level, it was important to have a more homogenous population of cells, before and after differentiation. Therefore, we chose to use OS25 ES cells that allow for G418 selection of undifferentiated (*Sox2* expressing) cells, and then selection against undifferentiated (*Oct4* expressing) cells with Ganciclovir after differentiation (Billon et al. 2002). The expression of alkaline phosphatase and SSEA-1 markers, and *Oct4*, confirmed the undifferentiated state of cells grown in the presence of LIF and G418 (Billon et al. 2002; data not shown). No expression of *Hoxb* genes was detected in these cells (Fig. 1B). Differentiation, induced by withdrawing LIF and adding RA, resulted in the complete loss of alkaline phosphatase and SSEA-1 markers and extinction of *Oct4* expression (Fig. 1B). After 2 to 4 d of differentiation (day 2 through 4), a robust pulse of *Hoxb1* expression was detected, but there was no expression of the more 5′ *Hoxb9* and *Hoxb13*. A pulse of *Hoxb9* expression was detected at day 10, at which time *Hoxb1* had been silenced (Fig. 1B). No *Hoxb13* expression was detected during the time course of the experiment. Therefore, we are able to recapitulate the sequence of expression from *Hoxb* in this ex vivo system, enabling us to follow the chromatin structure of the complex during induction.

Changes in histone H3 modification at Hoxb1 *and* Hoxb9

Transcriptionally active genes are generally characterized by high levels of histone acetylation and metH3-K4 (for review, see Zhang and Reinberg 2001; Lachner et al. 2003). We used ChIP and quantitative real-time PCR to examine changes in H3 modification at *Hoxb1* and *Hoxb9* before differentiation (neither gene expressed) and at day 4 (*Hoxb1* expressed) and day 10 (*Hoxb9* expressed) of differentiation. We also examined the r4 enhancer upstream of *Hoxb1*, which is required for its rhombomere 4 restricted expression (Popperl et al. 1995), and the RARE (3′DR2) located 1.2 kb 3′ of *Hoxb1* that mediates the early response to RA (Marshall et al. 1994; Fig. 2A). The presence of nucleosomes in these regions was confirmed by ChIP with antibody that detects the C terminus of H3 (Verreault et al. 1996). By day 4, increased H3 acetylated at K9 (AcH3-K9) was detected at all sites in *Hoxb1* and *Hoxb9* that were examined, even though only *Hoxb1* is expressed at this time. Levels of met_2H3-K4 also increased at *Hoxb1* by day 4 of differentiation, and surprisingly, constitutively high levels of this histone modification were found at exon 1 and the promoter of the silent *Hoxb9* both before and after differentiation. AcH3-K9 and met_2H3-K4 were lost from *Hoxb1* by day 10, when the gene has been silenced, but they persist at *Hoxb9* (Fig. 2B).

We conclude that RA rapidly induces histone modifications (AcH3-K9 and met_2H3-K4), which are considered as marks of active chromatin, at not only the 3′ end of the cluster where gene expression is induced at an early stage but also at more 5′ regions (*Hoxb9*). At these later sites, the changes in histone modifications precede transcriptional activation by many days. The subsequent loss of these histone modifications from *Hoxb1* parallels the cessation of *Hoxb1* expression. However, at no stage did we detect substantial levels of met_2H3-K9 (Fig. 2B), suggesting that this marker of gene repression is not important for the switch on or off of *Hoxb* expression in this system.

Chromatin decondensation at Hoxb

It has been suggested that an "opening" of chromatin structure may contribute to the regulation of *Hox* clusters (Van der Hoeven et al. 1996; Kondo and Duboule 1999; Roelen et al. 2002). Cytological chromatin decondensation accompanies transcriptional activation in some reporter systems (Tumbar et al. 1999; Tsukamoto et al. 2000; Muller et al. 2001). To determine if there are similar levels of chromatin decondensation accompanying induction of *Hoxb*, we measured the distance (d) between *Hoxb1* and *Hoxb9* hybridization signals in nuclei before and after RA induction. At probe separations of <2 Mb, there is a linear relationship between the mean-square interphase distances between them (d^2) and their separation in kilobases (van den Engh et al. 1992). This analysis has been used to show that different parts of the human genome have different levels of chromatin compaction (Yokota et al. 1997).

Hoxb1 and *Hoxb9* are 90 kb apart (Fig. 1A), and in nuclei of undifferentiated ES cells, they could barely be separated from one another. After day 2 of differentiation, they were readily separable in both MAA and pFa-fixed cells (Fig. 3A). Some recondensation of this region was then seen by day 10. The distribution of d values after day 2 conforms to a Rayleigh distribution (Sachs et al. 1995) ($SD/\langle d\rangle = 0.56$ and $median/\langle d\rangle = 0.9$) indicating

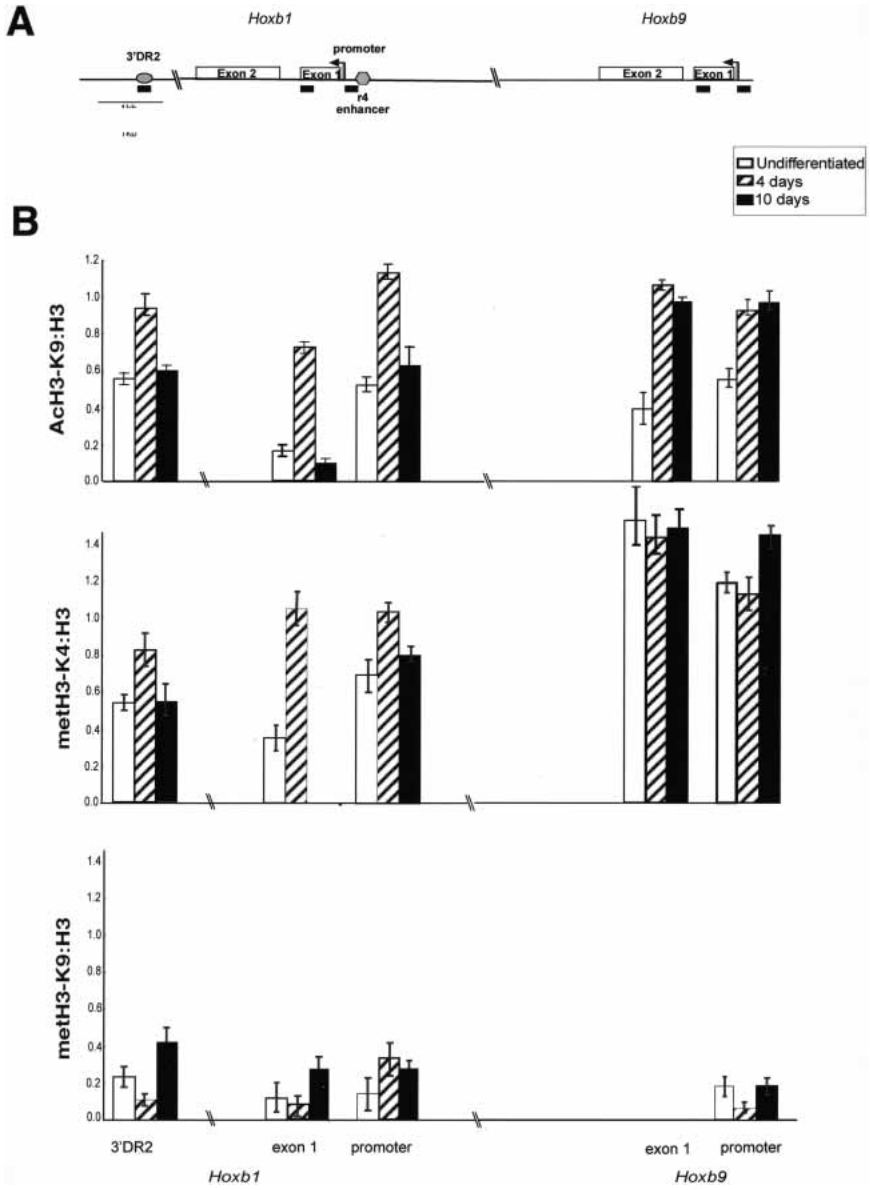

Figure 2. Histone H3 modifications upon induction of *HoxB* in ES cells. (*A*) Map of *Hoxb* and the elements analysed by ChIP. Exons of *Hoxb1* and *Hoxb9* are represented by two open bars. The arrows denote the transcription start sites of *Hoxb1* and *Hoxb9*. The 3′ RARE (3′DR2; Marshall et al. 1994) and the r4 enhancer (Popperl et al. 1995) are indicated by the filled bars. The position of the PCR products detected by ChIP are indicated by black bars underneath. (*B*) Quantification of ChIP by real-time PCR. The graphs show the mean levels of product amplified from samples after ChIP with antibodies recognizing AcH3-K9, met_2H3-K4, and met_2H3-K9 (after subtraction of mock IP levels) normalized relative to those obtained by ChIP with antibody recognizing the C terminus of H3. The analysis was carried out on chromatin prepared from undifferentiated ES cells (open bars) and from cells induced to differentiate with RA for 4 d (hatched bars) and 10 d (filled bars).

that the decondensed chromatin describes a random walk path.

Decondensation is not a general consequence of differentiation. The interphase separation between two control genes (*Rcn* and *Pax6*), the expression of which is not induced by RA and which are separated by 300 kb on MMU2, is not significantly different before and after 2 d of differentiation ($P = 0.46$; Fig. 3B).

The visual decondensation of *Hoxb* could represent a specific change in its higher-order chromatin structure or could just be a passive consequence of the increase in histone acetylation at the locus (Fig. 2) and its influence on folding of the chromatin fiber. To distinguish between these two possibilities, we experimentally increased histone acetylation in undifferentiated ES cells, by inhibiting the action of histone deacetylases (HDACs) with trichostatin A (TSA), in the absence of RA. Expression of *Hoxb* was determined by real-time RT–PCR. During the normal RA-induced differentiation program, there is an ~10-fold increase in the levels of *Hoxb1* mRNA by day 4. In contrast, only a very small (less than twofold) increase in *Hoxb1* mRNA was detected after exposure of undifferentiated ES cells to TSA, and there was no expression of *Hoxb9* (data not shown). TSA pretreatment does not prevent the normal execution of the program of RA-induced *Hoxb* expression because the correct sequence of *Hoxb1* and *Hoxb9* expression was seen at appropriate times after exposure of TSA-treated undifferentiated cells to RA (data not shown).

ChIP and real-time PCR showed that, in undifferentiated cells, TSA increased AcH3-K9 levels at *Hoxb1* and its regulatory elements to the same extent as that seen when untreated cells are differentiated with RA (data

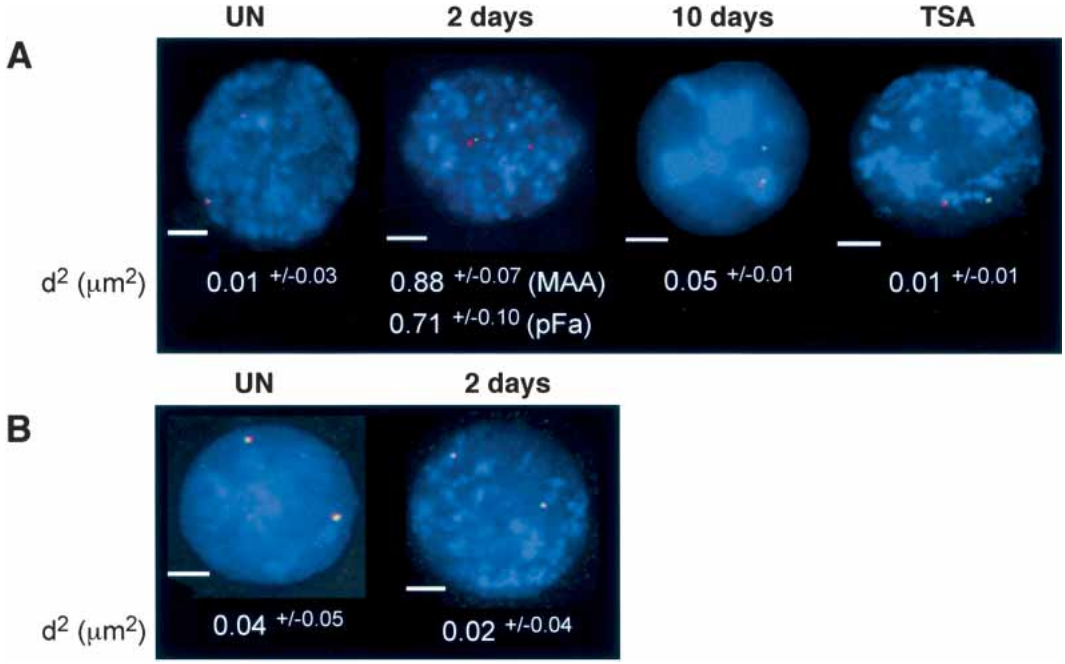

Figure 3. Decondensation of *Hoxb*. (*A*) FISH of *Hoxb1* (red) and *Hoxb9* (green) to MAA-fixed nuclei from undifferentiated (UN) cells, from cells at 2 or 10 d of differentiation, and from undifferentiated cells treated with TSA. Nuclei were counterstained with DAPI (blue). Bar, 5μm. Below it, each image the mean-square interprobe distance—d^2 (μm^2) ± S.E.M.—is shown (n = 50 cells). The value for cells at 2 d, fixed with pFa, is also shown. (*B*) FISH of Pax6 (red) and Rcn (green) probes on cells before and after (2 d) differentiation.

not shown). However, as well as no induction of *Hoxb* expression, there was no visual decondensation of the locus in TSA-treated cells (Fig. 3A). Therefore, we conclude that there is an approximate ninefold transient decondensation of the *Hoxb* complex upon induction with RA, and that this decondensation is not just a simple consequence of increased levels of histone acetylation.

Extrusion from the CT accompanies Hoxb *gene expression*

Although we have detected changes in histone modification and chromatin decondensation upon induction of *Hoxb*, the timing of these events early in the induction program (by day 4) does not account for the temporal program of gene expression—in particular, why is *Hoxb9* expression not seen until day 10? Domains of high transcriptional activity have been correlated with a distinctive chromatin structure at the cellular level, a looping out from CTs (Mahy et al. 2002a). Moreover, for some domains of coordinately regulated genes, the extrusion of these loops correlates with the up-regulation of gene expression (Volpi et al. 2000; Williams et al. 2002).

We therefore used FISH to examine how *HoxB* is organized relative to its CT, before and after induction. Probes encompassing *Hoxb1* or *Hoxb9* (Fig. 1A) and a paint for mouse chromosome 11 (MMU11) were cohybridized to nuclei from undifferentiated cells and from cells at day 4 or 10 of differentiation (Fig. 4A). We calculated the distance (in micrometers) between the *Hoxb* gene signals and the nearest CT edge as described previously (Fig. 4B; Table 1; Mahy et al. 2002a). In undifferentiated ES cell nuclei, most hybridization signals for both *Hoxb1* and *Hoxb9* were within the CT. By day 4 of differentiation, when *Hoxb1* is expressed, most of its hybridization signals are now located well (>0.2 μm) outside of the CT, but *Hoxb9* remains inside (Table 1; Fig. 4B,D). This was also confirmed by simultaneous detection of *Hoxb1*, *Hoxb9*, and MMU11 CT (Fig. 4C). A two-tailed distribution Student's t test showed that the relocalization of *Hoxb1* outside of the CT upon differentiation is statistically significant ($P < 0.000$). By day 10, *Hoxb1* expression is switched off and the gene relocalizes back toward the CT ($P = 0.02$;Fig. 4B,D). However, its location is still more exterior to the CT than in undifferentiated cells ($P < 0.000$). At day 10, Hoxb9 moves to the CT surface (Fig. 4D), and a significantly ($P = 0.001$) increased frequency of *Hoxb9* signals are now found outside of the CT, coincident with the expression of this gene (Fig. 4B; Table 1).

Relocalization outside the CT is not a general phenomena occurring upon differentiation, because the ubiquitously expressed *Rcn* gene locates inside of its MMU2 CT in both undifferentiated ES cells at all stages of differentiation (Fig. 4D; Mahy et al. 2002b). Consistent with the failure of TSA to induce chromatin decondensation at *HoxB*, we detected no movement of *Hoxb1* outside of the CT of TSA-treated cells. However, TSA treatment does not compromise subsequent induction because 2 d after RA induction of these cells, *Hoxb1* is expressed and loops out from the CT (Table 1).

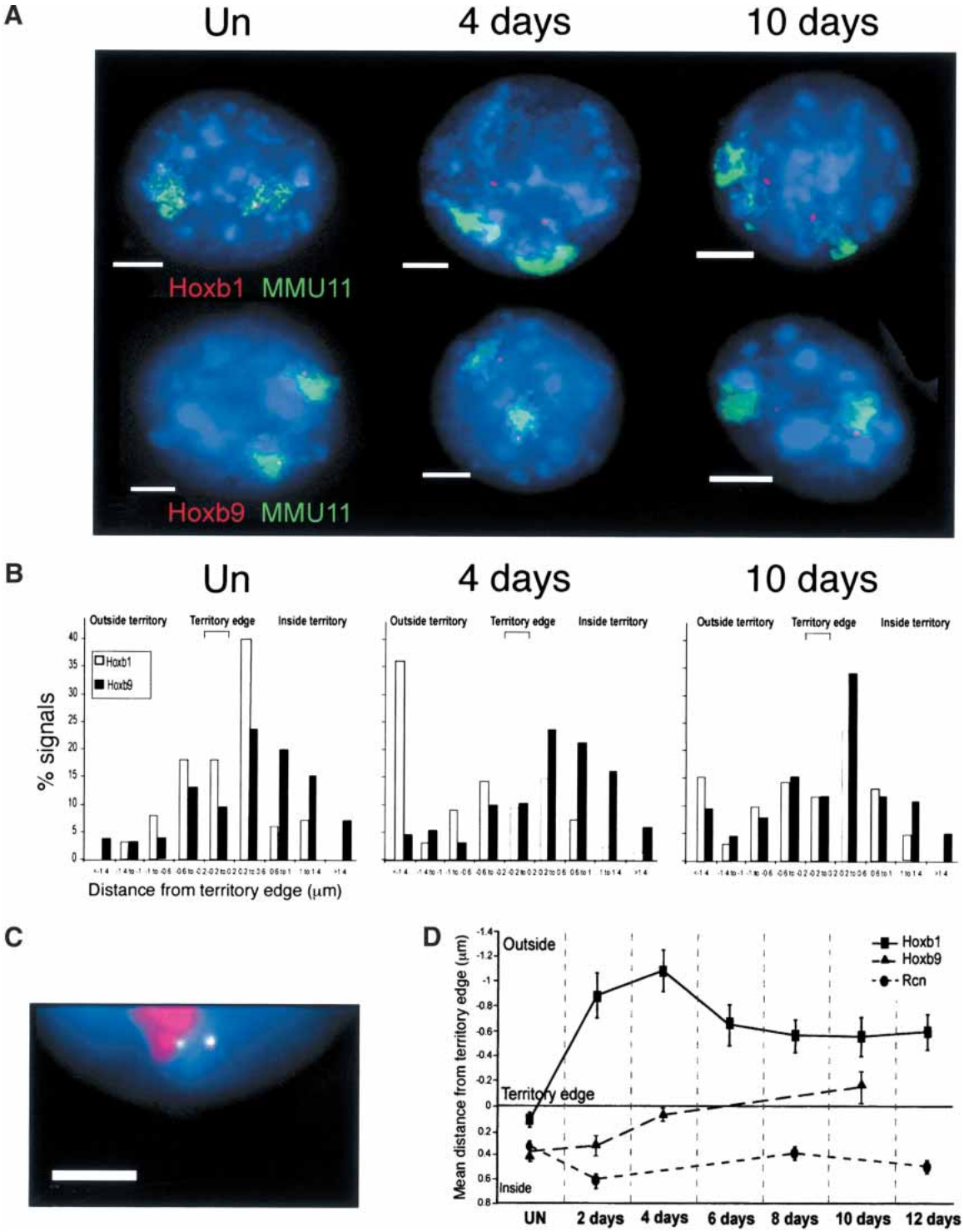

Figure 4. Progressive looping of the *HoxB* cluster from 3′ to 5′. (*A*) FISH with MMU11 chromosome paint (green) and gene-specific probes (red) for *Hoxb1* (*top*) or *Hoxb9* (*bottom*) on MAA-fixed nuclei from undifferentiated (UN) cells, and from cells at 4 or 10 d of differentiation. Nuclei were counterstained with DAPI (blue). Bars, 5 μm. (*B*) Histograms showing the distribution of hybridization signals for *Hoxb1* (open bars) or *Hoxb9* (filled bars) relative to the MMU11 territory edge (μm). Negative distances indicate signals located beyond the visible limits of the detectable CT. $n = 100$ territories. (*C*) FISH with MMU11 chromosome paint (red) and gene-specific probes for *Hoxb1* (green/red, 1:1) or *Hoxb9* (green) on nuclei from cells at 10 d of differentiation. Nuclei were counterstained with DAPI (blue). Bar, 5 μm. (*D*) Mean position (μm, ± S.E.M.) of *Hoxb1* and *Hoxb9* relative to the MMU11 territory edge during 12 d of differentiation. The position of *Rcn* in the MMU2 territory is shown as control (Mahy et al. 2002a). $n = 100$ territories. Normalization of the data to the size of the nucleus showed that the *Hoxb* movements are not due to the increased size of the nucleus and CT upon differentiation (data not shown).

Table 1. *Localization of* Hoxb *genes outside of CTs*

	% signals outside of MMU11 CT				
Gene	Undiff.	Day 4	Day 10	TSA	TSA + 2 d
Hoxb1 (MAA)	36	73	54	18	67
Hoxb1 (pFa)	15	65	N/D	N/D	N/D
Hoxb9 (MAA)	24	24	39	N/D	N/D

The percentage of *Hoxb1* or *Hoxb9* hybridization signals manually scored as being outside of the MMU11 CT by FISH to either MAA- or pFa-fixed nuclei from undifferentiated ES cells, and from cells after 4 and 10 d of differentiation. Undifferentiated cells that had been treated with TSA, and TSA-treated cells induced to differentiate with RA for 2 d, were also examined. N/D indicates not determined.

We conclude that in undifferentiated ES cells *Hoxb1* resides within, but close to, the surface of its CT. Upon induction with RA, it loops out away from the CT with kinetics that parallel those of its transcription, so that when *Hoxb1* expression is silenced after day 4, the frequency and extent of its looping decreases. However, it does not return to the same location as it was in before induction. Compared with *Hoxb1*, *Hoxb9* is located further inside of the CT in undifferentiated cells and remains there immediately after induction. Looping out of *Hoxb9* is not detected until day 10, and it never reaches the same extent as that seen for *Hoxb1* at day 4. Therefore, unlike the coordinate looping of the MHC (Volpi et al. 2000), the induction of expression from the *Hoxb* complex results in a progressive remodeling and a looping out of the region from the CT, which parallels the temporal activation of genes in the cluster.

Hoxb1 *moves toward the center of the nucleus upon induction*

Looping could just be a passive consequence of chromatin decondensation, or it could represent the recruitment of the locus to a particular region of the nucleus or nuclear compartment. In the former case, there need be no directionality to the movement relative to the center or the periphery of the nucleus. In the latter case, there may be directional movement. To test this, we determined the distribution of *Hoxb1* and *Hoxb9* hybridization signals in images of nuclei eroded into concentric shells, from the edge (shells 1 and 2) to the center (shells 4 and 5) of the nucleus (Croft et al. 1999). A significant ($P = 0.001$) movement of *Hoxb1* toward the nuclear center occurs at day 4 of differentiation, and by day 10, it has returned to its original nuclear location (Fig. 5). In contrast, there is a progressive movement of Hoxb9 toward the nuclear center between day 4 and 10 ($P = 0.008$; Fig. 5). There was no accompanying movement of the MMU11 CT in the same direction, suggesting that when *HoxB* loops out from the CT, it is specifically drawn toward the center of the nucleus.

Discussion

Changes in high-order chromatin structure and levels of gene expression

We have correlated the temporal pattern of gene expression from the *Hoxb* cluster with changes in nucleosome modification (Fig. 2), chromatin decondensation (Fig. 3), and an extrusion of *HoxB* genes out of the CT (Fig 4). We detect an increase (by day 4) of histone H3 acetylation (at

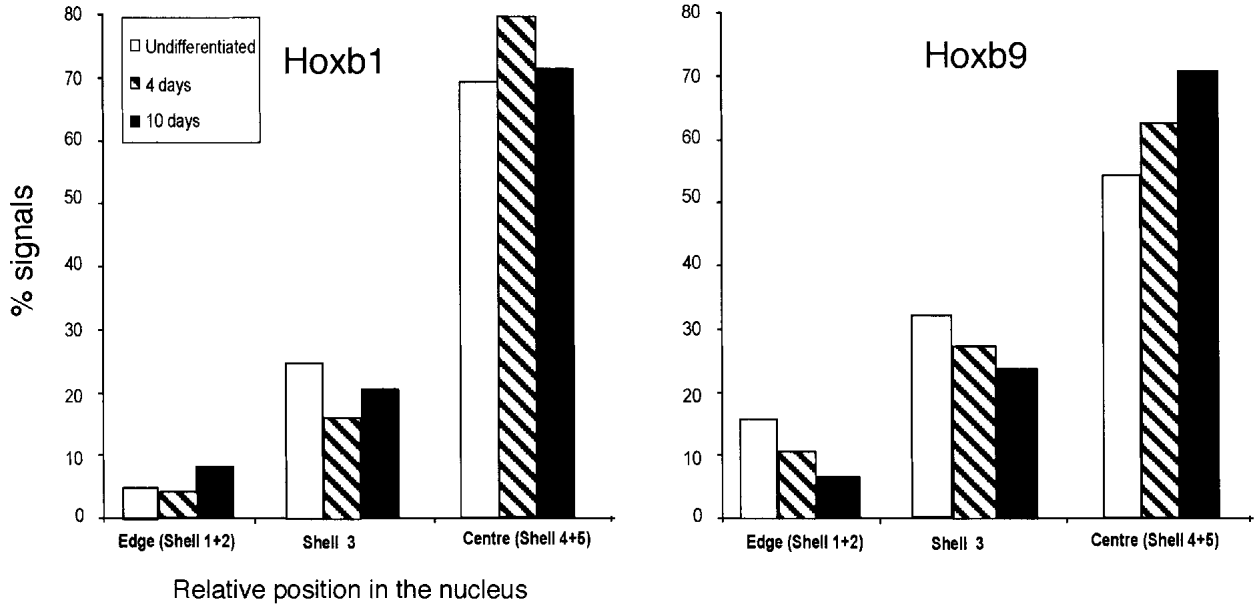

Figure 5. Movement of the *Hoxb1* toward the center of the nucleus. The localization of *Hoxb1* and *Hoxb9* hybridization signals within erosion shells from the edge (shells 1 and 2) toward the center (shells 4 and 5) of the nucleus. Analysis was performed on MAA-fixed nuclei from undifferentiated ES cells (open bars) and from cells after 4 and 10 d of differentiation (hatched and filled bars, respectively). $n = 50$ cells.

K9), and methylation of H3 at K4, upon induction by RA. This is consistent with the known associations of these histone marks with states of gene activation (Lachner et al. 2003). However, the modifications are gained at both the transcriptionally activated *Hoxb1* and at *Hoxb9*, which will remain silent for a further 6 d before its activation (Fig. 2). Therefore, these histone marks seem to be associated with poising of the genes for expression, rather than expression per se. We detect little met_2H3-K9 at *Hoxb1* or *Hoxb9*, no loss of met_2H3-K9 upon induction, and no acquisition of this histone modification when *Hoxb1* expression ceases after day 4. This suggests that this mark of gene repression is not involved in the early regulation of *HoxB*.

Although transcriptionally active chromatin is often considered to have an "open" chromatin structure, implying a decondensed chromatin structure, direct evidence for this has been lacking. Here we have shown for the first time that activation of an endogenous mammalian gene locus is accompanied by a visible approximately ninefold chromatin decondensation (Fig. 3). RA mediates its affects on *Hoxb* transcription via RA receptors that bind to RAREs such as the 3′DR2 (Marshall et al. 1994). Targeting of other nuclear hormone receptors to artificial arrays has also been shown to induce transient chromatin decondensation (Muller et al. 2001; Nye et al. 2002). However, compared with these studies, *HoxB* is several fold more decondensed, and the compaction is approximately consistent with formation of a 30-nm chromatin fiber

We have also shown that the induction of *Hoxb* expression is accompanied by a choreographed looping of the locus outside of CTs and toward the center of the nucleus, in a temporal pattern that parallels that of gene expression from the locus (Figs. 4, 5). Volpi et al. (2000) suggested that localization outside of CTs may be a visual manifestation of chromatin decondensation, and our data are consistent with this idea. Previously, we suggested that localization outside of CTs correlates with high levels of transcription (Mahy et al. 2002a). However, is it has also been suggested that looping outside of CTs can represent a poised state, prior to transcriptional activation (Ragoczy et al. 2003). In the very early embryo, prior to primitive streak formation, the 3′ end of *HoxB* is poised to respond to exogenous RA (Roelen et al. 2002). The rapid response to RA in ES cells (Fig. 1B; Papalopulu et al. 1991), and the absence of met_2H3-K9 prior to induction, suggests that *Hoxb1* is similarly poised for transcription in these cells. Because we have found that *Hoxb1* is inside of its CT in undifferentiated ES cells (Fig. 4), we suggest that the looping out of decondensed chromatin from the territory represents the transcriptionally active state and not a poised state (Fig. 6).

The mechanisms that mediated chromatin decondensation and extrusion from CTs have yet to be determined. It has been suggested that histone modifications may directly influence higher-order chromatin structures, for example, by altering nucleosome–DNA or nucleosome–nucleosome interactions, and by neutralizing charge in the histone N-terminal tails (Tse et al. 1998; Wolffe and Hayes 1999; Carruthers and Hansen 2000; Wang et al. 2001). However, increasing the levels of histone acetylation at *HoxB* experimentally with TSA does not lead to the changes in high-order chromatin structure that normally occur at the locus upon differentiation. Therefore, we suggest that chromatin compaction and nuclear organization represent a level of chromatin structure that is not simply a reflection of underlying histone acetylation.

Chromatin structure and the regulation of Hox *gene expression*

In vivo, *Hoxb1* expression is initiated in primitive streak mesoderm early in gastrulation (E7.2); however, *Hoxb1* and *Hoxb2*, but not more 5′ genes in the cluster, are poised to respond to exogenous RA before primitive streak formation (by E6.0; Roelen et al. 2002). In this regard, it is interesting to note that even in the nuclei of undifferentiated ES cells, the intrachromosomal organizations of *Hoxb1* and *Hoxb9* are different from each other. Whereas *Hoxb1* is located at the CT surface, *Hoxb9* is further inside the territory (Fig. 4D). The proximity of *Hoxb1* to the territory surface may contribute to its poised transcriptional state and may underlie its ability to respond rapidly and robustly to RA (Fig. 6). It will therefore be interesting to analyze the nuclear organization of *Hoxb1* when placed in inappropriate genomic locations (Kmita et al. 2000).

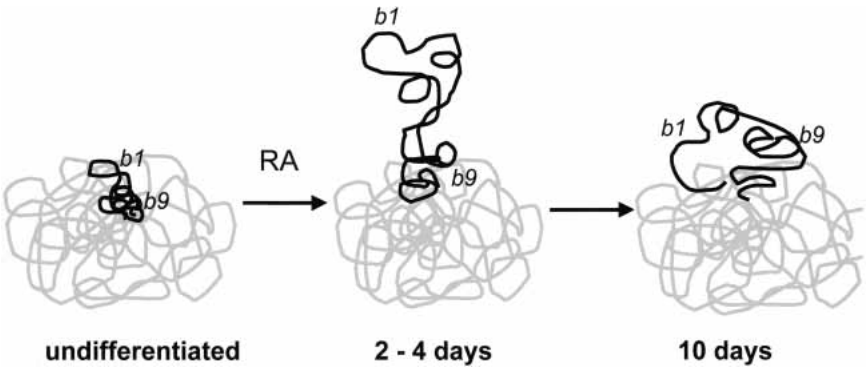

Figure 6. Changes in chromatin structure at *HoxB*. In undifferentiated ES cells, the entire *Hoxb* locus (black) is condensed with the MMU11 CT (gray). However, the 3′ *Hoxb1* gene is at the territory surface, poised to respond to retinoic acid (RA). The more 5′ *Hoxb9* is further inside the territory. After 2 d of induction with RA, the *Hoxb* chromatin fiber decondenses, and the 3′ end of the locus, including *Hoxb1*, is extruded from the CT. By 10 d of differentiation, *Hoxb1* is reeled in toward the CT, and *Hoxb9* has now left the CT.

We propose a two-step model through which chromatin structure regulates *Hoxb* expression (Fig. 6). In response to RA, there appears to be a widespread alteration in histone modification and chromatin condensation that is not restricted to the most 3′ gene (*Hoxb1*). We suggest that this establishes a transcriptionally competent chromatin state. The progressive looping out of genes from the CT may then contribute to the temporal pattern of gene expression and be necessary to support high rates of transcription. This later step, but not the first one, has similarities to models that propose that a (3′ to 5′) opening of chromatin structure that leads to the sequential accessibility of *Hox* genes for transcription (Van der Hoeven et al. 1996, Kondo and Duboule 1999; Roelen et al. 2002).

Materials and methods

ES cells culture, differentiation, and TSA treatment

Undifferentiated OS25 ES cells were maintained on 0.1% gelatin-coated dishes in Glasgows' minimal Eagle medium containing 10% fetal calf serum, nonessential amino acids, 1 mM sodium pyruvate, 0.3 mg/ml L-glutamine, 0.1 mM 2-mercaptoethanol, 1000 U/mL human recombinant LIF, and 100 µg/mL G418 (Billon et al. 2002).

To induce differentiation, 5×10^5 cells were plated in 25-cm^2 tissue culture flasks (Costar) without LIF or G418 for 1 d; 5×10^{-6} M RA was then added for 4 d. After 2 d (day 2 of differentiation) the cells were replated in 75-cm^2 flasks, and the RA-containing medium was supplemented with 2.5 µM Ganciclovir to select against undifferentiated cells for another 2 d (day 4). Subsequently, media was supplemented only with Ganciclovir (no RA) for eight more days until day 12. The medium was changed every 2 d during the differentiation protocol (Billon et al. 2002).

The 5×10^6 undifferentiated ES cells, maintained in medium supplemented with G418 and LIF, were treated with 160 nM TSA for 24 h.

Real-time RT–PCR

Twenty micrograms of total RNA, prepared by using Bio/RNA-X-cell (Bio/Gene Limited), were treated with 20 U Rnase-free DNase I (Promega). After phenol/chloroform extraction, the RNA was ethanol precipitated in 1 v of 5 M ammonium acetate and dissolved in H_2O. Two micrograms of RNA were reverse-transcribed by using Superscript II RNase H (Invitrogen) and 4 µL of Random Hexamers (50 µM; Amersham Pharmacia), and 1 µL was used as temple for real-time PCR, using the DNA-intercalating SYBR Green reagent and Master mix (Bio-Gene), on a lightcycler (Roche Molecular Biochemicals). Each reaction was performed in duplicate. PCR primers and conditions are described in Table 2. The 1:10, 1:100, and 1:1000 dilutions of β-actin PCR product of known concentration were used to produce a standard curve. The results were analyzed by Lightcycler software, version 3.5.

Chromatin immunoprecipitation

The ChIP protocol was modified from that of Christenson et al. (2001). ES cells were replated onto 10-cm tissue culture dishes. One day later, formaldehyde (Sigma), to a final concentration of 1%, was added to the medium for 10 min at room temperature. Cells were washed once in cold phosphate-buffered saline (PBS) before scraping in buffer A (85 mM KCl, 5.5% sucrose, 10 mM Tris at pH 7.5, 0.2 mM EDTA, 0.5 mM spermidine, 250 µM PMSF, and 1:100 protease inhibitor cocktail; Roche), containing

Table 2. *PCR primers and amplification conditions*

	Gene/locus	Primers	Product size (bp)	PCR conditions
RT–PCR	*Oct4*	GGCGTTCTCTTTGGAAAGGTGTTC CTCGAACCACATCCTTCTCT	312	15 min 95°C (30 sec 95°C, 30 sec 55°C; 30 sec 72°C) × 30
	Gapdh	CTCAAGATTGTCAGCAATGCA CCTTCCACAATGCCAAAGTT	70	15 min 95°C (30 sec 95°C, 30 sec 61°C, 25 sec 72°C) × 25
	Hoxb1	CCATATCCTCCGCCGCAG CGGACTGGTCAGAGGCATC	450	15 min 95°C (30 sec 95°C, 30 sec 62°C, 40 sec 72°C) × 35
	Hoxb9	CAGGGAGGCTGTCCTGTCTAATC CTTCTCTAGCTCCAGCGTCTGG	176	15 min 95°C (30 sec 95°C, 30 sec 68°C, 20 sec 72°C) × 30
	Hoxb13	CTGGAACAGCCAGATGTGTT CCTGCTAAAGGTGTCATCTC	445	15 min 95°C (30 sec 95°C, 30 sec 57°C, 40 sec 72°C) × 35
	β-actin	GGTCAGAAGGACTCCTATGTGG TCTCAGCTGTGTGGTGAAG	475	
ChIP	*Hob1* r4 + promoter + initiation site	TTCCATGTCGCTCTCAGATG TAGGAAGGGGCTAGGGAGTG	172	15 min 95°C (30 sec 95°C, 30 sec 64°C, 20 sec 72°C) × 25
	Hoxb1 3′DR2	GACAGTGGGTCCTGGGGGT GGTGCTCAACAGGCTTGTTTGGA	110	15 min 95°C (30 sec 95°C, 30 sec 61°C, 20 sec 72°C) × 25
	Hoxb1 exon 1	CCATATCCTCCGCCGCAG TCTGACGAGCAAGGCGATTCCTTG	104	
	Hoxb1 promoter	CCGCTTAGCCCATTGGCCT TAGGAAGGGGCTAGGGAGTG	80	
	Hoxb9 promoter	TCCGAAAGCCCTCTGCAC GACATTCTCAGACATTATCCGCG	110	
	Hoxb9 exon 1	GCACGCCCGAGTACAGTTTG CCTCTCTTTGTCCTCGCTTCCT	112	

0.5% NP40. The dish was rinsed with buffer A, and the cell suspension incubated for 5 min on ice and then centrifuged at 2000*g* for 3 min. The pellet was resuspended in 1% SDS, 10 mM EDTA, 50 mM Tris at pH8, and 250 µM PMSF and sonicated three times for 15 sec each at 10 µm of amplitude by using a Soniprep 150. Chromatin fragments were centrifuged for 3 min, 4°C, at 16000*g*, and the OD_{260nm} was measured. Ten micrograms of sonicated salmon sperm DNA (sssDNA) and 100 µL of protein G–agarose (Amersham Biosciences), prewashed two times in buffer A, were added to the supernatant and incubated for 1 h at 4°C on a rotating wheel. After centrifugation (2 min, 4°C, 2000*g*) to remove aggregated protein G, the supernatant was divided into aliquots of 150 µg DNA. One aliquot was kept aside (input), and one was incubated with no antibody as a negative control (mock IP).

Each test aliquot was diluted in 250 µL IP dilution buffer (100 mM Tris at pH 8, 150 mM NaCl, and 0.5% Triton X-100) and rotated overnight at 4°C with the following antibodies: 3 µL of antibody that recognizes the C terminus of H3 (Verreault et al. 1996), 5 µL anti-met_2H3-K4 (Upstate Biotechnology, 07-212), and anti-acH3-K9 (Upstate Biotechnology, 06-942) and anti-met_2H3-K9 (Abcam, ab7312). After antibody binding, 100 µg sssDNA and 100 µL 50% (v/v) protein G–agarose were added and incubated for 2 h at 4°C and then centrifuged for 2 min, 4°C, at 2000*g*. The chromatin-antibody/protein G–agarose complexes were washed for 5 min with 500 µL of each of the following buffers: IP dilution buffer, IP dilution buffer and 500 mM NaCl, wash buffer (10 mM Tris at pH 8.0, 500 mM LiCl, 1% NP40, and 1% deoxycholate), and TE (pH 8.0). One hundred microliters of TE (pH 8.0) with 500 µg/mL of RNaseA were added to the beads for 30 min at 37°C. Samples were eluted in 1% SDS and 0.1 M $NaHCO_3$. NaCl was added to 200 mM and the mixture heated for 6 h at 65°C to reverse the formaldehyde cross-links. Samples were digested with 20 µg/mL proteinase K for 1 h at 55°C and the DNA purified by phenol/chloroform extraction and ethanol precipitation. The DNA pellet was resuspended in 20 µL of sterile H_2O, and 1 µL aliquots were used as templates in real-time PCR.

PCR on immunoprecipitated DNA

One microliter of immunoprecipitated DNA was quantified by real-time PCR. For PCR in the 3′DR2 region and exon 1, DNA-intercalating SYBR Green reagent and The Master Mix (BioGene) was used. The QuantiTect SYBR Green PCR kit (Qiagen) was used for the *Hoxb1* and *Hoxb9* promoter. Each ChIP and each real-time PCR was done at least twice. Input sonicated DNA (150 µg) from ES cell lysate was diluted 1:10, 1:100, and 1:1000, and 1 µL amplified in parallel with the immunoprecipitated DNA (IP) to produce a standard curve. Each 10-fold dilution increased the C_T by about three cycles. For each amplification, the background corresponding to the mock IP was subtracted from the IP, and the specific enrichment was calculated from the standard curve.

FISH

Paint for mouse chromosome 2 (MMU2) was PCR-labeled with biotin-16-UTP as previously described (Mahy et al. 2002b). Biotin-16-UTP–labeled paint for MMU11 was purchased from Cambio. BACs 50j5 and 67L02 for *Rcn* and *Pax6*, respectively (Mahy et al. 2002b), were labeled with digoxigenin or biotin by nick-translation. The 50 kb BAC MMP-4 (T. Jinks, M.T. Martinez-Pastor, and R. Krumlauf, unpubl.) encompassing *Hoxb1* (Fig. 1A) was labeled with digoxigenin-11-dUTP by nick translation. A plasmid containing *Hoxb9* (P. Hunt and R. Krumlauf, unpubl.) was labeled with digoxigenin-11-dUTP or biotin-16-UTP. Approximately 200 ng of paint and 150 ng BAC/plasmid were used per slide, together with 15 µg mouse C*ot*1 DNA (GIBCO BRL) and 5 µg sssDNA.

Two-dimensional analysis was as described previously (Croft et al. 1999; Mahy et al. 2002b). To preserve three-dimensional nuclear structure, ES cells grown on slides were washed three times in PBS before permeabilization in CSK buffer (100 mM NaCl, 300 mM sucrose, 3 mM MgCl2, 10 mM PIPES at pH 6.8, and 0.5% Triton X100) for 5 min on ice. After washing three times in PBS, slides were fixed with 4% pFa/PBS for 10 min before freeze-thaw in 20% glycerol/PBS and FISH as described previously (Kurz et al. 1996; Mahy et al. 2002a,b).

Image analysis

Two-dimensional samples were examined on a Zeiss Axioplan fluorescence microscope fitted with a triple band-pass filter (Chroma no. 83000). Gray-scale images were captured with a cooled CCD camera (Princeton Instruments Pentamax) and custom IPLab scripts. For three-dimensional analysis, a focus motor was used to collect image stacks at 0.5-µm intervals along the z-axis. Images were captured with a Xillig CCD camera.

Analysis of probe position relative to CTs in 2D was as previously described (Mahy et al. 2002a,b). Because the size of the nucleus and the CTs increased upon differentiation, the locus to territory edge distance was also normalized by dividing it by the radius of the circle of equal area to that of the territory (Mahy et al. 2002b).

To calculate the d between two probes in two dimensions the hybridization signals were manually segmented and the xy coordinates of the centroid of each were determined. d was then calculated from $d = [(x_1 - x_2)^2 + (y_1 - y_2)^2]$. Calculation of d in stacks of three-dimensional images was similar. Briefly, the xyz coordinates of the centroid of each signal were determined. The distance between the two probes (or space diagonal) was the distance between two spots at opposite corner of a cuboid. $d_{abc} = (a^2 + b^2 + c^2)$; a, b, and c are the length of the side of the cuboid.

Probe position relative to the nuclear periphery and the nuclear center was determined by erosion of the nuclear area into five concentric shells (1 through 5) of equal area from the periphery of the nucleus to the center (Croft et al. 1999). The proportion of DAPI fluorescence and CT signal was calculated for each of the five shells, and the shell containing the gene signal was manually recorded. To do a *t* test for the gene probe, an arbitrary value was given to each shell (one at the periphery and five at the more center shells), and the number of probes located in each was multiplied by this value. To perform a *t* test for the CT position, the percentage of signal was multiplied by the mean radius for each shell. In a plane-projected sphere, the mean radius of random a point for each shell was calculated as $2/3[(r_b^3 - r_a^3)/(r_b^2 - r_a^2)]$.

Acknowledgments

S.C. was supported by fellowships from La Ligue Contre le Cancer and the Wellcome Trust (GR071481). W.A.B. is a Centennial fellow of the James S. McDonnell foundation. We thank Austin Smith (Institute for Stem Cell Research, Edinburgh) for OS25 cells, and Robb Krumlauf (Stowers Institute, Kansas City) for *Hoxb* BACs and for stimulating our research in this area. The H3-C terminal antibody was a gift of Alain Verreault (Cancer Research UK, Clare Hall). We are grateful to Nick Hastie, Robin Allshire, and Richard Meehan for critical reading of the manuscript.

The publication costs of this article were defrayed in part by payment of page charges. This article must therefore be hereby marked "advertisement" in accordance with 18 USC section 1734 solely to indicate this fact.

References

Andersson, K., Bjorkroth, B., and Daneholt, B. 1984. Packing of a specific gene into higher order structures following repression of RNA synthesis. *J. Cell. Biol.* **98:** 1296–1303.

Billon, N., Jolicoeur, C., Ying, Q.L., Smith, A., and Raff, M. 2002. Normal timing of oligodendrocyte development from genetically engineered, lineage-selectable mouse ES cells. *J. Cell. Sci.* **115:** 3657–3665.

Brown, D.G., Warren, V.N., Pahlsson, P., and Kimber, S.J. 1993. Carbohydrate antigen expression in murine embryonic stem cells and embryos, I: Lacto and neo-lacto determinants. *Histochem. J.* **25:** 452–463.

Bulger, M., Schubeler, D., Bender, M.A., Hamilton, J., Farrell, C.M., Hardison, R.C., and Groudine, M. 2003. A complex chromatin landscape revealed by patterns of nuclease sensitivity and histone modification within the mouse β-globin locus. *Mol. Cell. Biol.* **23:** 5234–5244.

Carruthers, L.M. and Hansen, J.C. 2000. The core histone N termini function independently of linker histones during chromatin condensation. *J. Biol. Chem.* **275:** 37285–37290.

Christenson, L.K., Stouffer, R.L., and Strauss III, J.F. 2001. Quantitative analysis of the hormone-induced hyperacetylation of histone H3 associated with the steroidogenic acute regulatory protein gene promoter. *J. Biol. Chem.* **276:** 27392–27399.

Croft, J.A., Bridger, J.M., Perry, P., Boyle, S., Teague, P., and Bickmore, W.A. 1999. Differences in the localization and morphology of chromosomes in the human nucleus. *J. Cell. Biol.* **145:** 1119–1131.

Dietzel, S., Schiebel, K., Little, G., Edelmann, P., Rappold, G.A., Eils, R., Cremer, C., and Cremer, T. 1999. The 3D positioning of ANT2 and ANT3 genes within female X chromosome territories correlates with gene activity. *Exp. Cell. Res.* **252:** 363–375.

Fischle, W., Wang, Y., and Allis, C.D. 2003. Histone and chromatin cross-talk. *Curr. Opin. Cell. Biol.* **15:** 172–183.

Gavalas, A. and Krumlauf, R. 2000. Retinoid signalling and hindbrain patterning. *Curr. Opin. Genet. Dev.* **10:** 380–386.

Hunt, P. and Krumlauf, R. 1992. Hox codes and positional specification in vertebrate embryonic axes. *Annu. Rev. Cell Biol.* **8:** 227–256.

Kim, A. and Dean, A. 2003. A human globin enhancer causes both discrete and widespread alterations in chromatin structure. *Mol. Cell. Biol.* **23:** 8099–8109.

Kmita, M. and Duboule, D. 2003. Organizing axes in time and space: 25 years of colinear tinkering. *Science* **301:** 331–333.

Kmita, M., van der Hoeven, F., Zakany, J., Krumlauf, R., and Duboule, D. 2000. Mechanisms of Hox gene colinearity: Transposition of the anterior Hoxb1 gene into the posterior HoxD complex. *Genes & Dev.* **14:** 198–211.

Kondo, T. and Duboule, D. 1999. Breaking colinearity in the mouse HoxD complex. *Cell* **97:** 407–417.

Kondo, T., Zakany, J., and Duboule, D. 1998. Control of colinearity in AdbB genes of the mouse HoxD complex. *Mol. Cell* **1:** 289–300.

Krumlauf, R. 1994. Hox genes in vertebrate development. *Cell* **78:** 191–201.

Kurz, A., Lampel, S., Nickolenko, J.E., Bradl, J., Benner, A., Zirbel, R.M., Cremer, T., and Lichter, P. 1996. Active and inactive genes localize preferentially in the periphery of chromosome territories. *J. Cell. Biol.* **135:** 1195–1205.

Lachner, M., O'Sullivan, R.J., and Jenuwein, T. 2003. An epigenetic road map for histone lysine methylation. *J. Cell. Sci.* **116:** 2117–2124.

Litt, M.D., Simpson, M., Gaszner, M., Allis, C.D., and Felsenfeld, G. 2001. Correlation between histone lysine methylation and developmental changes at the chicken β-globin locus. *Science* **293:** 2453–2455.

Maconochie, M.K., Nonchev, S., Studer, M., Chan, S.K., Popperl, H., Sham, M.H., Mann, R.S., and Krumlauf, R. 1997. Cross-regulation in the mouse HoxB complex: The expression of Hoxb2 in rhombomere 4 is regulated by Hoxb1. *Genes & Dev.* **11:** 1885–1895.

Mahy, N.L., Perry, P.E., and Bickmore, W.A. 2002a. Gene density and transcription influence the localization of chromatin outside of chromosome territories detectable by FISH. *J. Cell. Biol.* **159:** 753–763.

Mahy, N.L., Perry, P.E., Gilchrist, S., Baldock, R.A., and Bickmore, W.A. 2002b. Spatial organization of active and inactive genes and noncoding DNA within chromosome territories. *J. Cell. Biol* **157:** 579–589.

Marshall, H., Studer, M., Popperl, H., Aparicio, S., Kuroiwa, A., Brenner, S., and Krumlauf, R. 1994. A conserved retinoic acid response element required for early expression of the homeobox gene Hoxb-1. *Nature* **370:** 567–571.

Muller, W.G., Walker, D., Hager, G.L., and McNally, J.G. 2001. Large-scale chromatin decondensation and recondensation regulated by transcription from a natural promoter. *J. Cell. Biol.* **154:** 33–48.

Nye, A.C., Rajendran, R.R., Stenoien, D.L., Mancini, M.A., Katzenellenbogen, B.S., and Belmont, A.S. 2002. Alteration of large-scale chromatin structure by estrogen receptor. *Mol. Cell. Biol.* **22:** 3437–3449.

Oosterveen, T., Niederreither, K., Dolle, P., Chambon, P., Meijlink, F., and Deschamps, J. 2003. Retinoids regulate the anterior expression boundaries of 5′ Hoxb genes in posterior hindbrain. *EMBO J.* **22:** 262–269.

Papalopulu, N., Lovell-Badge, R., and Krumlauf, R. 1991. The expression of murine Hox-2 genes is dependent on the differentiation pathway and displays a collinear sensitivity to retinoic acid in F9 cells and *Xenopus* embryos. *Nucl. Acids Res.* **19:** 5497–5506.

Popperl, H., Bienz, M., Studer, M., Chan, S.K., Aparicio, S., Brenner, S., Mann, R.S., and Krumlauf, R. 1995. Segmental expression of Hoxb-1 is controlled by a highly conserved autoregulatory loop dependent upon exd/pbx. *Cell* **81:** 1031–1042.

Ragoczy, T., Telling, A., Sawado, T., Groudine, M., and Kosak, S.T. 2003. A genetic analysis of chromosome territory looping: Diverse roles for distal regulatory elements. *Chrom. Res.* **11:** 513–525.

Roelen, B.A.J., de Graaff, W., Forlani, S., and Deschamps, J. 2002. Hox cluster polarity in early transcriptional availability: A high order regularity level of clustered Hox genes in the mouse. *Mech. Develop.* **119:** 81–90.

Sachs, R.K., Van den Engh, G., Trask, B., Yokota, H., and Hearst, J.E. 1995. A random-walk/giant-loop model for interphase chromosomes. *Proc. Natl. Acad. Sci.* **92:** 2710–2714.

Schubeler, D., Francastel, C., Cimbora, D.M., Reik, A., Martin, D.I., and Groudine, M. 2000. Nuclear localization and histone acetylation: A pathway for chromatin opening and transcriptional activation of the human β-globin locus. *Genes & Dev.* **14:** 940–950.

Simeone, A., Acampora, D., Arcioni, L., Andrews, P.W., Boncinelli, E., and Mavilio, F. 1990. Sequential activation of

HOX2 homeobox genes by retinoic acid in human embryonal carcinoma cells. *Nature* **346:** 763–766.
Simeone, A., Acampora, D., Nigro, V., Faiella, A., D'Esposito, M., Stornaiuolo, A., Mavilio, F., and Boncinelli, E. 1991. Differential regulation by retinoic acid of the homeobox genes of the four *HOX* loci in human embryonal carcinoma cells. *Mech. Develop.* **33:** 215–227.
Studer, M., Gavalas, A., Marshall, H., Ariza-McNaughton, L., Rijli, F.M., Chambon, P., and Krumlauf, R. 1998. Genetic interactions between Hoxa1 and Hoxb1 reveal new roles in regulation of early hindbrain patterning. *Development* **125:** 1025–1036.
Tse, C., Sera, T., Wolffe, A.P., and Hansen, J.C. 1998. Disruption of higher-order folding by core histone acetylation dramatically enhances transcription of nucleosomal arrays by RNA polymerase III. *Mol. Cell. Biol.* **18:** 4629–4638.
Tsukamoto, T., Hashiguchi, N., Janicki, S.M., Tumbar, T., Belmont, A.S., and Spector, D.L. 2000. Visualization of gene activity in living cells. *Nat. Cell. Biol.* **2:** 871–878.
Tumbar, T., Sudlow, G., and Belmont, A.S. 1999. Large-scale chromatin unfolding and remodeling induced by VP16 acidic activation domain. *J. Cell. Biol.* **145:** 1341–1354.
van den Engh, G., Sachs, R., and Trask, B.J. 1992. Estimating genomic distance from DNA sequence location in cell nuclei by a random walk. *Science* **257:** 1410–1412.
Van der Hoeven, F., Zakany, J., and Duboule, D. 1996. Gene transpositions in the HoxD complex reveal a hierarchy of regulatory controls. *Cell* **85:** 1025–1035.
Verreault, A., Kaufman, P.D., Kobayashi, R., and Stillman, B. 1996. Nucleosome assembly by a complex of CAF-1 and acetylated histones H3/H4. *Cell* **87:** 95–104.
Volpi, E.V., Chevret, E., Jones, T., Vatcheva, R., Williamson, J., Beck, S., Campbell, R.D., Goldsworthy, M., Powis, S.H., Ragoussis, J., et al. 2000. Large-scale chromatin organisation of the major histocompatibility complex and other regions of human chromosome 6 and its response to interferon in interphase nuclei. *J. Cell. Sci.* **113:** 1565–1576.
Wang, X., He, C., Moore, S.C., and Ausio, J. 2001. Effects of histone acetylation on the solubility and folding of the chromatin fiber. *J. Biol. Chem.* **276:** 12764–12768.
Williams, R.R.E., Broad, S., Sheer, D., and Ragoussis, J. 2002. Subchromosomal positioning of the epidermal differentiation complex (EDC) in keratinocyte and lymphoblast interphase nuclei. *Exp. Cell. Res.* **272:** 163–175.
Wolffe, A.P. and Hayes, J.J. 1999. Chromatin disruption and modification. *Nucl. Acids Res.* **27:** 711–720.
Ye, Q., Hu, Y.F., Zhong, H., Nye, A.C., Belmont, A.S., and Li, R. 2001. BRCA1-induced large-scale chromatin unfolding and allele-specific effects of cancer-predisposing mutations. *J. Cell. Biol.* **155:** 911–921.
Yokota, H., Singer, M.J., van den Engh, G.J., and Trask, B.J. 1997. Regional differences in the compaction of chromatin in human G_0/G_1 interphase nuclei. *Chrom. Res.* **5:** 157–166.
Zhang, Y. and Reinberg, D. 2001. Transcription regulation by histone methylation: Interplay between different covalent modifications of the core histone tails. *Genes & Dev.* **15:** 2343–2360.